IOP PUBLISHING JOURNAL OF PHYSICS: CONDENSED MATTER

J. Phys.: Condens. Matter **19** (2007) 356004 (12pp) doi:10.1088/0953-8984/19/35/356004

First-principles calculations of $BaZrO_3$(001) and (011) surfaces

R I Eglitis

Department of Materials Science and Engineering, Sung Kyun Kwan University, 440-746 Suwon, Korea
and
Institute of Solid State Physics, University of Latvia, Riga LV1063, Latvia

Received 26 April 2007, in final form 19 June 2007
Published 8 August 2007
Online at stacks.iop.org/JPhysCM/19/356004

Abstract

In an extension of our previous studies of $BaTiO_3$, $SrTiO_3$, and $PbTiO_3$(001), as well as $BaTiO_3$ and $SrTiO_3$(011) surfaces [1–6], I present and discuss the results of calculations of $BaZrO_3$(001) surface relaxation and rumpling with two different terminations (BaO and ZrO_2), and $BaZrO_3$(011) polar surface relaxation with three terminations (Ba-, ZrO- and O-terminated, A-type). These are based on hybrid Hartree–Fock and density-functional theory exchange functionals, using Becke's three-parameter method, combined with the nonlocal correlation functionals by Perdew and Wang [7]. According to the results of my calculations, all upper layer atoms for ZrO_2- and BaO-terminated $BaZrO_3$(001) surfaces relax inwards. The surface rumpling for the BaO-terminated $BaZrO_3$(001) surface is much larger than for the ZrO_2-terminated $BaZrO_3$(001) surface. Both BaO-terminated (1.30 eV) and ZrO_2-terminated (1.31 eV) surfaces are stable and energetically equally favourable. Unlike the $BaZrO_3$(001) surface, different terminations of the (011) surface lead to great differences in the surface energies. The A-type O-terminated surface has the lowest energy (2.32 eV). The Ba-terminated $BaZrO_3$(011) surface has a much higher surface energy of 2.90 eV, while the $BaZrO_3$ ZrO-terminated (011) surface has the highest energy (3.09 eV). I predict a considerable increase of the Zr–O chemical bond covalency near the (011) surface, as compared to both the bulk and the (001) surface.

(Some figures in this article are in colour only in the electronic version)

1. Introduction

The ABO_3 perovskite surfaces have numerous technological applications, including high-capacity memory cells, catalysis, optical wave guides, integrated optics applications, and as substrates for high-T_c cuprate superconductor growth, [8–10], for which the surface structure and quality are of primary importance. Considering the high technological importance of

 © 2007 IOP Publishing Ltd Printed in the UK

ABO_3 perovskites, it is not surprising that, during recent years, their (001) surfaces have been the subject of many theoretical studies by means of *ab initio* and classical shell model (SM) methods [11–20]. The $SrTiO_3$(001) surface relaxation has been experimentally studied by means of low-energy electron diffraction (LEED), reflection high-energy electron diffraction (RHEED), medium-energy ion scattering (MEIS), and surface x-ray diffraction (SXRD) measurements [21–25].

In general, the results of the LEED experiments [21] agree quite well with the results of *ab initio* and shell model calculations. Note, however, that the LEED [21] and RHEED [22] experiments contradict each other in the sign (reduction or expansion) of the interplane distances between the top metal and the second crystal layers (Δd_{12}) for the SrO-terminated $SrTiO_3$(001) surface. Another problem is that LEED, RHEED, and MEIS experiments argue that the topmost O atoms always move outwards from the surface whereas all calculations predict for the TiO_2-terminated $SrTiO_3$(001) surface that the O atoms go *inwards*. The reason for this is not clear and is discussed in [11, 25]. Even more important is a clear contradiction between the three above-mentioned experiments and a recent SXRD [25] experiment in which oxygen atoms are predicted to move *inwards* for both TiO_2- and SrO-terminated $SrTiO_3$(001) surfaces, reaching 12.5% of the lattice constant for the TiO_2-terminated surface.

The $SrTiO_3$(011) polar perovskite surface was studied experimentally using several different techniques. Low-energy electron diffraction shows a number of surface reconstructions at high temperatures, and atomic force microscopy also supports surface modification due to applied extensive thermal treatment [26–28]. However, there are no experimental estimates of the surface relaxation of the $SrTiO_3$ or $BaZrO_3$(011) surfaces at low temperatures, with which I could compare my calculations.

It is surprising that, despite the high technological potential, there are no experimental and theoretical studies reported dealing with $BaZrO_3$(011) surfaces. In order to fill this gap, and taking into account that the predictive power of first-principles quantum electronic structure calculations due to increased speed of computers and recent developments of new and powerful computational methods allows for the rational design on paper of new materials and their properties for technology applications, I performed *ab initio* calculations for $BaZrO_3$ surfaces. It is the aim of the present paper to provide an application of state-of-the-art first-principles methods to the (011) polar termination of $BaZrO_3$, which is the first such report to the best of my knowledge.

2. Computational method

To perform the first-principles DFT-B3PW calculations, I used the CRYSTAL computer code [7]. This code employs the Gaussian-type functions (GTFs) localized at atoms as the basis for an expansion of the crystalline orbitals. The features of the CRYSTAL code which are most important for this study are its ability to calculate the electronic structure of materials within both Hartree–Fock (HF) and Kohn–Sham (KS) Hamiltonians. My calculations were performed using the hybrid exchange–correlation B3PW functional involving a hybrid of non-local Fock exact exchange, local density approximation (LDA) exchange and Becke's gradient-corrected exchange functional [29], combined with the nonlocal gradient-corrected correlation potential by Perdew and Wang [30–32]. The Hay–Wadt small-core effective core pseudopotentials (ECPs) were adopted for the Ba atom [33]. The 'small-core' ECPs replace only inner core orbitals, but orbitals for sub-valence electrons as well as for valence electrons are calculated self-consistently. Light oxygen atoms were treated with the all-electron basis set.

The reciprocal space integration was performed by sampling the Brillouin zone of the unit cell with an $8 \times 8 \times 1$ Pack–Monkhorst net [34], which provides a balanced summation in

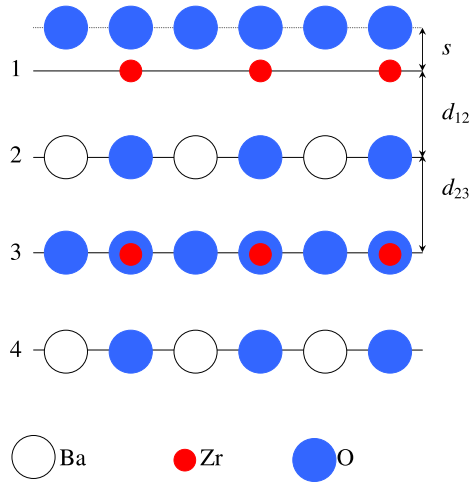

Figure 1. Side view of a ZrO_2-terminated $BaZrO_3(001)$ surface with the definitions of the surface rumpling s and the near-surface interplane distances d_{12} and d_{23}, respectively.

direct and reciprocal spaces [35]. To achieve high accuracy, large enough tolerances of 7, 8, 7, 7, 14, were chosen for the Coulomb overlap, Coulomb penetration, exchange overlap, the first exchange pseudo-overlap, and the second exchange pseudo-overlap, respectively [7]. The $BaZrO_3(001)$ surfaces were modelled with two-dimensional (2D) slabs, consisting of several planes perpendicular to the [001] crystal direction. The CRYSTAL code allowed me to avoid artificial periodicity along the Oz direction and to perform simulations for stand-alone 2D slabs. To simulate $BaZrO_3(001)$ surfaces, I used symmetrical (with respect to the mirror plane) slabs consisting of seven alternating ZrO_2 and BaO layers. One of these slabs was terminated by BaO planes and consisted of a supercell containing 17 atoms. The second slab was terminated by ZrO_2 planes and consisted of a supercell containing 18 atoms. These slabs are non-stoichiometric, with unit cell formulae $Ba_4Zr_3O_{10}$ and $Ba_3Zr_4O_{11}$, respectively. These two (BaO and ZrO_2) terminations are the only two possible flat and dense (001) surfaces in $BaZrO_3$ perovskite lattice structure. The sequence of layers with [001] orientation in $BaZrO_3$ is illustrated in figure 1. An alternative asymmetrical 8-layer $BaZrO_3(001)$ slab is BaO- and ZrO_2-terminated (from each side, respectively) and stoichiometric with unit cell formula $Ba_4Zr_4O_{12}$. According to our previous study dealing with $SrTiO_3$, $BaTiO_3$ and $PbTiO_3(001)$ surfaces [2, 6], the atomic displacements obtained for asymmetrically terminated (stoichiometric) slabs containing 8 layers and 20 atoms and symmetrically terminated (non-stoichiometric) slabs containing 7 layers and 17 or 18 atoms, respectively, are practically the same. This means that both symmetrical (non-stoichiometric) and asymmetrical (stoichiometric) slabs are reliable for the calculations of the $BaZrO_3(001)$ neutral surface. Therefore I chose for my current calculations either BaO- or ZrO_2-terminated symmetrical (non-stoichiometric) $BaZrO_3(001)$ slabs containing 7 layers and 17 or 18 atoms, respectively.

Unlike the $BaZrO_3(001)$ neutral surface, the problem in modelling the $BaZrO_3(011)$ polar surface is that it consists of charged planes, O–O or BaZrO. If one assumes fixed ionic charges O^{2-}, Zr^{4+}, and Ba^{2+}, then modelling of the $BaZrO_3(011)$ surface exactly as would be obtained from a perfect crystal cleavage leads either to an infinite macroscopic dipole moment perpendicular to the surface, when the slab is terminated by planes of different kinds (O_2 and

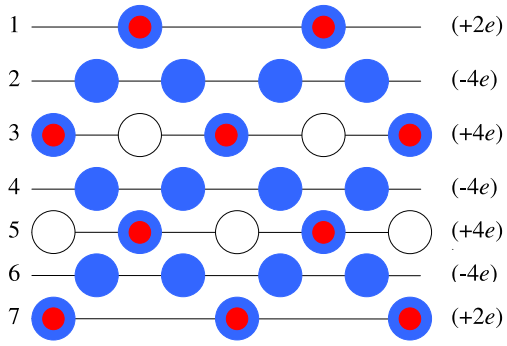

Figure 2. ZrO-terminated $BaZrO_3(011)$ surface.

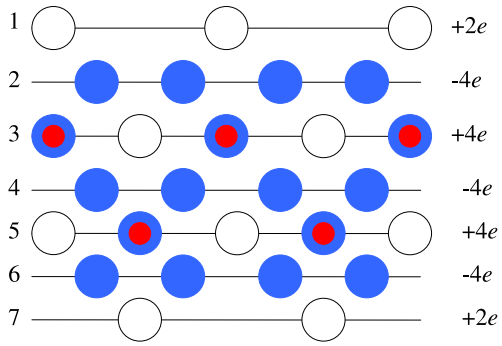

Figure 3. Ba-terminated $BaZrO_3(011)$ surface.

BaZrO) (stoichiometric slab), or to infinite charge, when it is terminated by the same type of crystalline planes (O_2–O_2 or BaZrO–BaZrO) (non-stoichiometric slab). It is known that such crystal terminations make the surface unstable [36, 37]. In real quantum-chemical calculations for a finite-thickness slab terminated by the different kind of planes (stoichiometric slab) the charge redistribution near the surface arising during the self-consistent field (SCF) procedure could, in principle, compensate the macroscopic dipole moment. On the other hand, in the calculations of non-stoichiometric slabs terminated by similar planes the charge neutrality could be retained by setting in the computer inputs an appropriate number of electrons or just zero net charge of the unit cell. Nevertheless, careful studies for another ABO_3 perovskite, $SrTiO_3$ [36, 38, 39], demonstrate that these two options for $SrTiO_3$ surfaces are energetically expensive with respect to the dipole moment elimination via the introduction of vacancies.

This was the reason why in my $BaZrO_3(011)$ surface calculations, in order to get the neutral slab, I removed the O atom from the upper and lower layers of the 7-layer symmetric O–O-terminated non-stoichiometric slab, and Ba or both Zr and O atoms from the upper and lower layers of the BaZrO-terminated non-stoichiometric slab. Thereby, in my calculations, the ZrO-terminated symmetric 7-layer non-stoichiometric slab consisted of a supercell containing 16 atoms (see figure 2), and finally, the Ba- and O-terminated symmetric non-stoichiometric 7-layer slabs consisted of supercells containing 14 and 15 atoms, respectively (see figure 3 and figure 4). Stoichiometric and non-stoichiometric (011) surface terminations, and the number of bonds cleaved, are discussed very comprehensively for the related ABO_3 perovskite $SrTiO_3$ in [39].

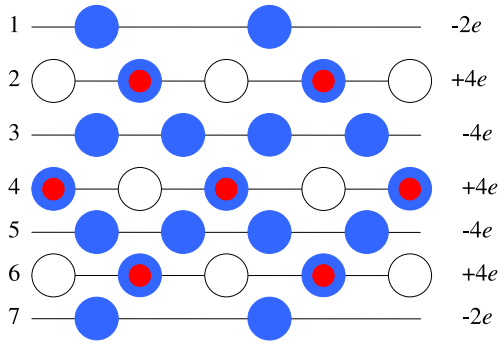

Figure 4. Side view of O-terminated $BaZrO_3$(011) surface, configuration A.

Table 1. Effective charges and bond populations of atoms in $BaZrO_3$ bulk.

Ion	Property	B3PW calculation
Ba^{2+}	Charge Q (in e)	+1.815
	Bond populations P (in me)	−12
O^{2-}	Charge Q (in e)	−1.316
	Bond populations P (in me)	108
Zr^{4+}	Charge Q (in e)	+2.134

Table 2. Atomic relaxation of the uppermost three layers (in per cent of lattice constant) for the ZrO_2-terminated $BaZrO_3$(001) surface calculated by the hybrid B3PW method. Positive (negative) values refer to displacements in the direction outwards from (inwards to) the surface.

N	Ion	B3PW (Δz% of a_o)
1	Zr^{4+}	−1.79
	O^{2-}	−1.70
2	Ba^{2+}	+1.94
	O^{2-}	+0.85
3	Zr^{4+}	−0.03
	O^{2-}	0.00

3. Calculated results for $BaZrO_3$ bulk and (001) surface atomic and electronic structure

As a starting point for my calculations, I calculated the $BaZrO_3$ lattice constant (4.234 Å). To characterize the chemical bonding and covalency effects, I used a standard Mulliken population analysis for the effective atomic charges Q and other local properties of electronic structure (bond orders, atomic covalencies and full valencies) as described, for example, in [40, 41]. My calculated effective charges are (+1.815e) for the Ba atom, (+2.134e) for the Zr atom, and (−1.316e) for the O atom. The bond population of the chemical bonding between Zr and O atoms is (+108 me), but bond populations between O and O atoms (−8 me), and between Ba and O atoms (−12 me) are negative, which indicates repulsion between O–O atoms (see table 1). The negative bond populations between Ba and O atoms is within the error bars of the CRYSTAL code. Similar negative bond populations between Sr and O atoms were also obtained for $SrTiO_3$ [3–5].

The atomic displacements obtained by me using the B3PW method for ZrO_2- and BaO-terminated $BaZrO_3$(001) surfaces are shown in tables 2 and 3. According to the results of

Table 3. Atomic relaxation of the uppermost three layers (in per cent of lattice constant) for the BaO-terminated $BaZrO_3(001)$ surface calculated by the hybrid B3PW method. Positive (negative) values refer to displacements in the direction outwards from (inwards to) the surface.

N	Ion	B3PW ($\Delta z\%$ of a_o)
1	Ba^{2+}	−4.30
	O^{2-}	−1.23
2	Zr^{4+}	+0.47
	O^{2-}	+0.18
3	Ba^{2+}	−0.01
	O^{2-}	−0.14

Table 4. The calculated surface rumpling s and relative displacements (Δd_{ij}) for the three near-surface planes of BaO- and ZrO_2-terminated (001) surfaces (in per cent of bulk lattice constant).

	BaO-terminated			ZrO_2-terminated		
Method	s	Δd_{12}	Δd_{23}	s	Δd_{12}	Δd_{23}
B3PW	3.07	−4.77	+0.48	0.09	−3.73	+1.97

my calculations, atoms of the first surface layer relax inwards, i.e. towards the bulk, for both ZrO_2- and BaO-terminated $BaZrO_3(001)$ surfaces. The outward relaxation of all atoms in the second layer is found for both terminations of the $BaZrO_3(001)$ surface. Displacements of the third-layer atoms were found to be negligibly small in my calculations.

In order to compare the calculated surface structures with experimental results, the surface rumpling s (the relative displacement of oxygen with respect to the metal atom in the surface layer) (see figure 1) and the changes in interlayer distances Δd_{12} and Δd_{23} (1, 2, and 3 are the numbers of near-surface layers) are presented in table 4. My calculations of the interlayer distances are based on the positions of relaxed metal ions (figure 1), which are known to be much stronger electron scatterers than oxygen ions [21]. From table 4 one can see that both $BaZrO_3(001)$ surfaces show the reduction of interlayer distance Δd_{12} and expansion of Δd_{23}. The relaxation of the upper layer surface metal atoms is much larger than that of oxygen ions for the BaO-terminated $BaZrO_3(001)$ surface, which leads to a considerable *rumpling* of the outermost plane (see table 4). The amplitude of surface rumpling of the BaO-terminated $BaZrO_3(001)$ surface is predicted to be considerably larger than that for the ZrO_2-terminated $BaZrO_3(001)$ surface.

Atomic displacements, the effective static charges, and bond populations between nearest metal and oxygen atoms are given in table 5. The major effect observed here is strengthening of the Zr–O chemical bond near the surface. Note that the Zr and O effective charges in the $BaZrO_3$ bulk (+2.134e and −1.316e, respectively) are much smaller than those expected in an ionic model; furthermore the Zr–O bond is considerably populated (108 me, m = milli). The Zr–O bond population for the ZrO_2-terminated $BaZrO_3(001)$ surface is 132 me (see table 5), which is considerably larger than the relevant values in the bulk. In contrast, the Ba–O bond populations are very small and even negative, which indicates repulsion. This effect is also well seen from the Ba effective charges, which is close to the formal ionic charge of +2e.

In order to calculate the $BaZrO_3(001)$ surface energy, I start with the cleavage energy for unrelaxed BaO- and ZrO_2-terminated surfaces. In my calculations the two 7-layer BaO- and ZrO_2-terminated slabs, containing 17 and 18 atoms, respectively, represent together 7 bulk unit cells containing 5 atoms. Surfaces with both terminations arise simultaneously under cleavage

Table 5. Calculated absolute magnitudes of atomic displacements D (in Å), the effective atomic charges Q (in e) and bond populations P between nearest Me–O atoms (in me) for the ZrO_2- and BaO-terminated ZrO_2 (001) surfaces.

ZrO_2-terminated $BaZrO_3$ surface				BaO-terminated $BaZrO_3$ surface			
Layer no	Ion	Property	B3PW	Layer no	Ion	Property	B3PW
1	Zr^{4+}	D	−0.075 7886	1	Ba^{2+}	D	−0.182 062
		Q	+2.173			Q	+1.779
		P	132			P	−8
	O^{2-}	D	−0.071 9780		O^{2-}	D	−0.052 078
		Q	−1.239			Q	−1.491
		P	−18			P	44
2	Ba^{2+}	D	+0.082 1396	2	Zr^{4+}	D	+0.0198 998
		Q	+1.797			Q	+2.189
		P	−10			P	90
	O^{2-}	D	+0.035 989		O^{2-}	D	+0.007 6212
		Q	−1.273			Q	−1.356
		P	106			P	−12
3	Zr^{4+}	D	−0.001 2702	3	Ba^{2+}	D	−0.000 4234
		Q	+2.133			Q	+1.811
		P	116			P	−12
	O^{2-}	D	0		O^{2-}	D	−0.005 9276
		Q	−1.30			Q	−1.328
		P	−12			P	104
Bulk	Zr^{4+}	Q	+2.134	Bulk	Zr^{4+}	Q	+2.134
		P	108			P	108
	O^{2-}	Q	−1.316		O^{2-}	Q	−1.316
		P	−12			P	−12
	Ba^{2+}	Q	+1.815		Ba^{2+}	Q	+1.815

of the crystal and the relevant cleavage energy is distributed equally between created surfaces. Therefore, I assume that the cleavage energy is the same for both terminations:

$$E_s^{(unrel)} = \tfrac{1}{4}[E_{slab}^{(unrel)}(BaO) + E_{slab}^{(unrel)}(ZrO_2) - 7E_{bulk}], \quad (1)$$

where $E_{slab}^{(unrel)}(BaO)$ and $E_{slab}^{(unrel)}$ (ZrO_2) are unrelaxed BaO- and ZrO_2-terminated slab energies, E_{bulk} is energy per bulk unit cell, and the factor of 4 comes from the fact that I create four surfaces upon the cleavage procedure. According to the results of my calculations, the total energy for the unrelaxed BaO-terminated $BaZrO_3(001)$ slab is equal to −27 057.055 779 eV, the total energy for the unrelaxed ZrO_2-terminated $BaZrO_3(001)$ slab is equal to −29 685.733 014 eV, and finally, the total energy for the $BaZrO_3$ bulk unit cell containing 5 atoms is equal to −8106.947 442 eV. Next, I can calculate the relaxation energies for each of BaO and ZrO_2 terminations, when both sides of the slabs relax:

$$E_{rel}(A) = \tfrac{1}{2}[E_{slab}(A) - E_{slab}^{(unrel)}(A)]; \quad (2)$$

$E_{slab}(A)$ is the slab energy after relaxation, and A = BaO or ZrO_2. According to the results of my calculations the total energy of the BaO-terminated $BaZrO_3(001)$ slab after the relaxation of atoms is equal to −27 057.387 826 eV, and the total energy for the ZrO_2-terminated $BaZrO_3(001)$ slab after the relaxation of atoms is equal to −29 686.028 657 eV. Lastly, the surface energy sought for is just a sum of the cleavage and relaxation energies:

$$E_s(A) = E_s^{(unrel)} + E_{rel}(A). \quad (3)$$

Table 6. Calculated surface energies (in eV per surface cell) for BaO- and ZrO_2-terminated $BaZrO_3(001)$ surfaces.

Termination	Surface energy
BaO	1.30
ZrO_2	1.31

In order to calculate the $BaZrO_3(011)$ surface energy for the ZrO- and Ba-terminated surfaces, containing 16 and 14 atoms, respectively, I start with the cleavage energy for unrelaxed surfaces. In my calculations for $BaZrO_3(011)$ surfaces the two 7-plane Ba- and ZrO-terminated slabs represent together six bulk unit cells. The surfaces with both terminations arise simultaneously under cleavage of the crystal, and the relevant cleavage energy is divided equally between these two surfaces. Therefore, I assume that the cleavage energy is the same for both terminations:

$$E_s^{(unrel)} = \tfrac{1}{4}[E_{slab}^{(unrel)}(Ba) + E_{slab}^{(unrel)}(ZrO) - 6E_{bulk}], \tag{4}$$

where $E_{slab}^{(unrel)}(Ba)$ and $E_{slab}^{(unrel)}(ZrO)$ are energies of the unrelaxed slabs, E_{bulk} is the energy per bulk unit cell, and $\frac{1}{4}$ means that in total four surfaces were created upon the crystal cleavage. My calculated total energies for unrelaxed Ba- and ZrO-terminated $BaZrO_3(011)$ surfaces are equal to −21 681.880 527 eV and −26 941.831 973 eV, respectively. Next I calculate the relaxation energies $E_{rel}(A)$ using equation (2) for each of the Ba- and ZrO-terminated surfaces, when both sides of slabs are allowed to relax. In the case for the $BaZrO_3(011)$ surface A = Ba or ZrO. According to the results of my calculations, after the relaxation of atoms for Ba- and ZrO-terminated $BaZrO_3(011)$ surfaces the total energy of system is equal to −21 685.066 116 eV and −26 944.644 617 eV, respectively. Finally, the surface energy $E_s(A)$ sought for is just a sum of the cleavage and relaxation energies (3). When I cleave the $BaZrO_3$ crystal in another way, I obtain two identical O-terminated surfaces, containing 15 atoms. This allows me to simplify the calculations. Note that the unit cell of the 7-plane O-terminated slab contains three bulk unit cells. Therefore, the relevant surface energy is

$$E_s(O, A) = \tfrac{1}{2}[E_{slab}(O, A) - 3E_{bulk}], \tag{5}$$

where $E_s(O, A)$ and $E_{slab}(O, A)$ are the surface energy and the slab total energy for the O-terminated surface in the asymmetric configuration A. According to the results of my calculations, the total energy of the O-terminated $BaZrO_3(011)$ surface in the asymmetric configuration after the relaxation of atoms is equal to −24 316.206 750 eV. Additional details dealing with the related ABO_3 perovskite $SrTiO_3$ surface energy calculations are given in [39].

The results of calculations for the surface energy of relaxed BaO- and ZrO_2-terminated $BaZrO_3(001)$ surfaces are presented in table 6. According to my calculations the E_s value for the BaO termination (1.30 eV/cell) is slightly smaller than for the ZrO_2 termination (1.31 eV/cell). However, the surface energy difference is small, and both surfaces are stable and energetically equally favourable.

4. Calculated results for $BaZrO_3(011)$ surface atomic and electronic structures

Table 7 gives the surface energies, calculated using the hybrid B3PW method. Unlike the $BaZrO_3(001)$ surface, I see that different terminations of the (011) surface lead to great differences in the surface energies. Here the lowest energy is that of the A-type O-terminated surface (2.32 eV/cell). My calculated surface energy for the ZrO-terminated

Table 7. Surface energies (in electron volts per unit cell area) for the three different $BaZrO_3(011)$ terminations calculated using the hybrid B3PW method. In both cases three near-surface planes were relaxed.

Termination	Surface energy
Ba	2.90
ZrO	3.09
O-terminated, A-type	2.32

Table 8. Atomic relaxation of the $BaZrO_3(011)$ surface (in per cent of the lattice constant) for the three terminations, calculated by means of the *ab initio* B3PW method. A positive sign corresponds to outward atomic displacements (towards the vacuum).

Layer number	Ion	B3PW, Δz	B3PW, Δy
	Zr–O-terminated		
1	Zr^{4+}	−6.61	
1	O^{2-}	+3.35	
2	O^{2-}	−0.29	
3	Ba^{2+}	−1.51	
3	O^{2-}	−3.54	
3	Zr^{4+}	+0.90	
	Ba-terminated		
1	Ba^{2+}	−11.81	
2	O^{2-}	+0.66	
3	Zr^{4+}	+0.09	
3	O^{2-}	−0.07	
3	Ba^{2+}	+0.71	
	O-terminated, A-type		
1	O^{2-}	−7.32	−1.54
2	Zr^{4+}	+0.12	−2.36
2	Ba^{2+}	+0.21	+2.43
2	O^{2-}	−0.78	+8.27
3	O^{2-}	−0.07	+0.43

$BaZrO_3(011)$ surface (3.09 eV/cell) is larger than that for the Ba-terminated $BaZrO_3(011)$ surface (2.90 eV/cell).

The hybrid B3PW calculated atomic relaxations for $BaZrO_3(011)$ surfaces are shown in table 8. An idea of the nature of the relaxed (011) surfaces can be obtained from figures 2–4 (see front views). The first layer metal atoms for ZrO- and Ba-terminated $BaZrO_3(011)$ surfaces relax strongly inwards, by $0.0661a_o$ for Zr and by $0.1181a_o$ for Ba, whereas the O atoms on the ZrO-terminated (011) surface relax outwards by $0.0335a_o$. The O atoms in the top layer of the A-type O-terminated surface also move inwards by $0.0732a_o$. The Zr atoms in the second layer of this surface move along the surface, by $0.0236a_o$, and also slightly outwards. The atomic displacements in the third plane from the surface for the three terminations of $BaZrO_3(011)$ surfaces are still large. This is in sharp contrast with my results for the neutral $BaZrO_3(001)$ surfaces (see tables 2 and 3), where the atomic displacements converge very quickly and are already small in the third layer.

The interatomic bond populations for the three possible terminations are given in table 9. The major effect observed here is a strong increase of the Zr–O chemical bonding (152 me)

Table 9. The A–B bond populations P (in milli e = me) and the relevant interatomic distances R (in Å) for the three different (110) terminations in $BaZrO_3$. Symbols I–IV denote the number of each plane enumerated from the surface. The nearest-neighbour Zr–O distance in the unrelaxed lattice is 2.117 Å.

Atom A	Atom B	P	R
	ZrO-terminated		
Zr(I)	O(I)	152	2.159
	O(II)	252	1.937
O(II)	Zr(III)	130	2.082
	Ba(III)	−4	3.020
	O(III)	2	2.994
Zr(III)	Ba(III)	0	3.668
	O(III)	130	2.082
	O(IV)	130	2.125
Ba(III)	O(III)	−12	2.995
	O(IV)	−14	2.962
O(III)	O(IV)	−24	2.922
	Ba-terminated		
Ba(I)	O(II)	−46	2.768
O(II)	Ba(III)	−14	2.993
	Zr(III)	82	2.134
	O(III)	−26	2.994
Ba(III)	O(III)	−12	2.994
	O(IV)	−10	3.009
Zr(III)	O(III)	70	2.117
	Ba(III)	−2	3.667
	O(IV)	130	2.120
O(III)	O(IV)	−8	2.992
	O-terminated, A-type		
O(I)	Ba(II)	−36	2.763
	Zr(II)	154	1.880
	O(II)	20	3.102
Ba(II)	O(II)	−30	2.747
	Zr(II)	−2	3.503
Zr(II)	O(II)	102	2.165
	O(III)	176	1.982
O(II)	O(III)	8	3.108
Ba(II)	O(III)	−10	3.002
O(III)	O(IV)	−18	2.940
	Zr(IV)	128	2.040
	Ba(IV)	−6	3.048

near the ZrO-terminated $BaZrO_3$(011) surface as compared to already large bonding in the bulk (108 me) and near the ZrO_2-terminated $BaZrO_3$(001) surface (132 me). For the O-terminated A-type (011) surface the O(I)–Zr(II) bond population is as large as 154 me, i.e., by a factor of 1.5 larger than that in the bulk.

5. Conclusions

According to the results of my calculations, all upper layer atoms for ZrO_2- and BaO-terminated $BaZrO_3$(001) surfaces relax inwards. In (001) surface, the displacement of Ba on the BaO-

terminated surface is larger than that of Zr atom on the ZrO_2-terminated surface. The surface rumpling for BaO-terminated $BaZrO_3(001)$ surface is much larger than for the ZrO_2-terminated $BaZrO_3(001)$ surface. My calculations predict a compression of the distance between the first and second planes, and an expansion for the second and third planes.

I found that the relaxation magnitudes of the Ba- and ZrO-terminated $BaZrO_3(011)$ surface upper layer metal atoms are stronger than for the $BaZrO_3(001)$ surface upper layer atoms. Whereas the metal atoms on the Ba- and ZrO-terminated $BaZrO_3(011)$ surfaces relax strongly inwards, the oxygen atoms on the ZrO-terminated $BaZrO_3(011)$ surface upper layer relax outwards by 3.35% of the lattice constant a_o.

Both BaO-terminated (1.30 eV) and ZrO_2-terminated (1.31 eV) surfaces are stable and energetically equally favourable. Unlike the $BaZrO_3(001)$ surface, I see that different terminations of the (011) surface lead to great differences in the surface energies. Here the lowest energy is that of the A-type O-terminated surface (2.32 eV). My calculated surface energies of Ba-terminated (2.90 eV) and ZrO-terminated (3.09 eV) $BaZrO_3(011)$ surfaces is more than two times larger than those of BaO- and ZrO_2-terminated $BaZrO_3(001)$ surfaces.

I found that relaxation of the $BaZrO_3(011)$ surfaces for all three terminations is considerably stronger than for (001) surfaces. The atomic displacements in the third plane from the surface for the three terminations of $BaZrO_3(011)$ surfaces are still large. This is in sharp contrast with my results for the neutral $BaZrO_3(001)$ surfaces, where the atomic displacements converge very quickly and are already small in the third layer. My *ab initio* calculations indicate a considerable increase of the Zr–O bond covalency (152 m*e*) near the $BaZrO_3(011)$ surface relative to $BaZrO_3$ bulk (108 m*e*), much larger than that for the (001) surface (132 m*e*).

Acknowledgments

The author gratefully acknowledges partial financial support by the Latvian Research Programmes No 05.1704 and Programme on Materials Science.

References

[1] Eglitis R I, Borstel G, Heifets E, Piskunov S and Kotomin E 2006 *J. Electroceram.* **16** 289
[2] Eglitis R I, Piskunov S, Heifets E, Kotomin E A and Borstel G 2004 *Ceram. Int.* **30** 1989
[3] Heifets E, Eglitis R I, Kotomin E A, Maier J and Borstel G 2001 *Phys. Rev.* B **64** 235417
[4] Heifets E, Goddard W A, Kotomin E A, Eglitis R I and Borstel G 2004 *Phys. Rev.* B **69** 035408
[5] Heifets E, Eglitis R I, Kotomin E A, Maier J and Borstel G 2002 *Surf. Sci.* **513** 211
[6] Piskunov S, Kotomin E A, Heifets E, Maier J, Eglitis R I and Borstel G 2005 *Surf. Sci.* **575** 75
[7] Saunders V R, Dovesi R, Roetti C, Causa M, Harisson N M, Orlando R and Zicovich-Wilson C M 2003 *CRYSTAL-2003 User Manual* (Italy: University of Torino)
[8] Noguera C 1996 *Physics and Chemistry at Oxide Surfaces* (Cambridge: Cambridge University Press)
[9] Liness M E and Glass A M 1977 *Principles and Applications of Ferroelectrics and Related Materials* (Oxford: Clarendon)
[10] Auciello O, Scott J F and Ramesh R 1998 *Phys. Today* **22** (July)
[11] Padilla J and Vanderbilt D 1998 *Surf. Sci.* **418** 64
[12] Padilla J and Vanderbilt D 1997 *Phys. Rev.* B **56** 1625
[13] Meyer B, Padilla J and Vanderbilt D 1999 *Faraday Discuss.* **114** 395
[14] Cora F and Catlow C R A 1999 *Faraday Discuss.* **114** 421
[15] Cohen R E 1997 *Ferroelectrics* **194** 323
[16] Fu L, Yaschenko E, Resca L and Resta R 1999 *Phys. Rev.* B **60** 2697
[17] Cheng C, Kunc K and Lee M H 2000 *Phys. Rev.* B **62** 10409
[18] Heifets E, Dorfman S, Fuks D and Kotomin E 1997 *Thin Solid Films* **296** 76
[19] Heifets E, Dorfman S, Fuks D, Kotomin E and Gordon A 1998 *J. Phys.: Condens. Matter* **10** L347
[20] Erdman N, Poeppelmeler K, Asta M, Warschakov O and Ellis D E 2002 *Nature* **419** 55

[21] Bickel N, Schmidt G, Heinz K and Müller K 1989 *Phys. Rev. Lett.* **62** 2009
[22] Hikita T, Hanado T, Kudo M and Kawai M 1993 *Surf. Sci.* **287/288** 377
[23] Kudo M, Hikita T, Hanade T, Sekine R and Kawai M 1994 *Surf. Interface Anal.* **22** 412
[24] Kido Y, Nishimura T, Hoshido Y and Mamba H 2000 *Nucl. Instrum. Methods Phys. Res.* **161–163** 371
[25] Charlton G, Brennan S, Muryn C A, McGrath R, Norman D, Turner T S and Thorton G 2000 *Surf. Sci.* **457** L376
[26] Szot K and Speier W 1999 *Phys. Rev.* B **60** 5909
[27] Bando H, Ochiai Y, Aiura Y, Haruyama Y, Yasue T and Nishihara Y 2001 *J. Vac. Sci. Technol.* A **19** 1938
[28] Brunen J and Zegenhagen J 1997 *Surf. Sci.* **389** 349
[29] Becke A D 1993 *J. Chem. Phys.* **98** 5648
[30] Perdew J P and Wang Y 1986 *Phys. Rev.* B **33** 8800
[31] Perdew J P and Wang Y 1989 *Phys. Rev.* B **40** 3399
[32] Perdew J P and Wang Y 1992 *Phys. Rev.* B **45** 13244
[33] Piskunov S, Heifets E, Eglitis R I and Borstel G 2004 *Comput. Mater. Sci.* **29** 165
[34] Monkhorst H J and Pack J D 1976 *Phys. Rev.* B **13** 5188
[35] Bredow T, Evarestov R A and Jug K 2000 *Phys. Status Solidi* b **222** 495
[36] Noguera C 2000 *J. Phys.: Condens. Matter* **12** R367
[37] Tasker P W 1979 *J. Phys. C: Solid State Phys.* **12** 4977
[38] Pojani A, Finocchi F and Noguera C 1999 *Surf. Sci.* **442** 179
[39] Bottin F, Finocchi F and Noguera C 2003 *Phys. Rev.* B **68** 035418
[40] Catlow C R A and Stoneham A M 1983 *J. Phys. C: Solid State Phys.* **16** 4321
[41] Bochiccio R C and Reale H F 1993 *J. Phys. B: At. Mol. Opt. Phys.* **26** 4871